

The orthogonal fitting procedure for determination of the empirical $\Sigma - D$ relations for supernova remnants: application to starburst galaxy M82

D. Urošević^{1,2}, B. Vukotić,³ B. Arbutina¹, and M. Sarevska⁴

ABSTRACT

The radio surface brightness-to-diameter ($\Sigma - D$) relation for supernova remnants (SNRs) in the starburst galaxy M82 is analyzed in a statistically more robust manner than in the previous studies that mainly discussed sample quality and related selection effects. The statistics of data fits in $\log \Sigma - \log D$ plane are analyzed by using vertical (standard) and orthogonal regressions. As the parameter values of $D - \Sigma$ and $\Sigma - D$ fits are invariant within the estimated uncertainties for orthogonal regressions, slopes of the empirical $\Sigma - D$ relations should be determined by using the orthogonal regression fitting procedure. Thus obtained $\Sigma - D$ relations for samples which are not under severe influence of the selection effects could be used for estimating SNR distances. Using the orthogonal regression fitting procedure $\Sigma - D$ slope $\beta \approx 3.9$ is obtained for the sample of 31 SNRs in M82. The results of implemented Monte Carlo simulations show that the sensitivity selection effect does not significantly influence the slope of M82 relation. This relation could be used for estimation of distances to SNRs that evolve in denser interstellar environment, with number density up to 1000 particles per cm^3 .

Subject headings: galaxies: individual (M82) — ISM: supernova remnants — methods: statistical — radio continuum: ISM

1. Introduction

The relation between surface brightness Σ and diameter D for supernova remnants (SNRs) - known as the $\Sigma - D$ relation - is a standard way for investigating the radio brightness evolution of these sources. In the vast majority of situations it is not feasible to observe the detailed evolution of individual SNRs over very long periods of time. However by studying the properties of samples of SNRs, which cover a range of different ages but are assumed to follow similar evolutionary paths, it is possible to analyze their statistical properties and evolution. Understanding the statistical and evolutionary properties of SNR samples and particularly using well defined samples to determine the $\Sigma - D$ relation also has an important role in providing a method of distance determination for individual SNRs. This is particularly relevant for Galactic SNRs, of which more than 200 have unknown or ill-determined distance measures (see for example, Green 2009).

In a single external galaxy all SNRs in the sample are at essentially the same distance. This makes the extragalactic samples of better quality when compared to Galactic ones, because the problems stemming

¹Department of Astronomy, Faculty of Mathematics, University of Belgrade, Studentski trg 16, 11000 Belgrade, Serbia; dejanu@math.rs, arbo@math.rs

²Isaac Newton Institute of Chile, Yugoslavia Branch

³Astronomical Observatory, Volgina 7, 11060 Belgrade 38, Serbia; bvukotic@aob.rs

⁴University of Niš, Serbia

from inaccurate knowledge of distances are eliminated. Additionally, Malmquist bias¹ severely acts in the Galactic samples making them incomplete. An extragalactic sample is not influenced by Malmquist bias. On the other hand, the best radio instruments at this moment can provide detection of brighter SNRs only in the nearby galaxies. Such a limited survey sensitivity results in a selection effect that significantly reduces the number of detected objects within a relatively distant extragalactic system (approximately up to 15 Mpc, see Urošević et al. 2005, hereafter Paper I and Chomiuk & Wilcots 2009).

This paper presents a fitting procedure that can result, if reliable samples are used, in $\Sigma - D$ relations that are more useful in terms of distance estimation. The usual form of the relation is:

$$\Sigma = AD^{-\beta}, \quad (1)$$

where parameter A and slope β are obtained by fitting of the observational data for a sample of SNRs.

The two initial empirical $\Sigma - D$ relations were derived by Poveda & Woltjer (1968) and Milne (1970). During the 1970's and early 1980's a number of detailed analyzes of Galactic relations were presented (eg. Clark & Caswell 1976, Milne 1979). More critical analysis started with the work of Green (1984). A Galactic $\Sigma - D$ relation that is still quite frequently used was derived by Case & Bhattacharya (1998). A brief review of Galactic and extragalactic relations was presented by Urošević (2002). The updated Galactic $\Sigma - D$ relations were derived by Guseinov et al. (2003) and Xu, Zhang & Han (2005).

The best sample for the $\Sigma - D$ analysis consists of compact SNRs from starburst galaxy M82 (see Arbutina et al. 2004 and Paper I). The analyzed sample (21 SNRs) was taken from Huang et al. (1994) and McDonald et al. (2002). This sample is different than other Galactic and extragalactic samples because it has the steepest $\Sigma - D$ slope (see Paper I) and shows a relatively high degree of $L - D$ correlation (for more on $L - D$ correlation and trivial $\Sigma - D$ relation concept, see Arbutina et al. 2004). Furthermore, unlike other samples, it consists of a relatively high number of very small and very bright SNRs (Paper I, Fenech et al. 2008, hereafter F08). It is important to note that in an extragalactic sample all the SNRs are essentially at the same distance, wherefore a uniformly sensitive survey has a uniform sensitivity in luminosity, or surface brightness for all SNRs within the sample. The survey sensitivity selection effect has weaker influence on the M82 $\Sigma - D$ slope than on the slopes derived for other nearby galaxies because M82 SNRs are of relatively high brightness. This is shown in Paper I on Monte Carlo generated artificial extragalactic samples; after generating the sample, a sensitivity cutoff is applied selecting only the points above the survey sensitivity line. The apparent (after selection) and true (before selection) fitted slopes of the simulated samples are then compared with the slopes fitted to the real data.

In this paper we use the new observations of compact SNRs in M82 by F08. From F08, we extract data set that consists of 31 SNRs and fit $\Sigma - D$ regression for both orthogonal and vertical offsets. Additionally, Monte Carlo simulations are performed to illustrate the selection effect of survey sensitivity on the fitted $\Sigma - D$ slopes for M82 sample (the simulation algorithm is explained in more details in Section 5).

¹The volume selection effect – intrinsically bright objects are favored in any flux limited survey because they are sampled from a larger spatial volume.

2. The M82 data sample

All data analyzed herein are collected from F08. The central kpc of M82 was mapped at 5 GHz using MERLIN². The largest detectable angular size with this array at 5 GHz is ~ 1.2 arc seconds (18.5 pc at the distance of M82). Fenech et al. present new MERLIN observation made in 2002 along with observations made ten years earlier which previously published by Muxlow et al 1994. Depending on particular image parameters, the angular resolution in 1992 and 2002 data varies in the range 35 – 50 mas (0.54 – 0.78 pc), but all sources were resolved with 35 mas beam (F08). Also, the rms noise in the 2002 data images varies in the range 17 – 24 μJybeam^{-1} and 46 – 60 μJybeam^{-1} for the 1992 data images (F08).

The sources from 2002 observation are listed in Table 2 of F08. Out of 55 sources there are 36 SNRs. For the purpose of this paper, we have excluded five SNRs with the largest angular size diameter estimates (sources with peak flux $\lesssim 0.1$ mJy beam⁻¹). Inspection of Figure 3 in F08 shows that these five sources are mostly of non-compact structure with only the brightest parts above the sample sensitivity limit (0.085 mJy beam⁻¹). Consequently, these sources are easily confused with noise and the diameters of their faint extended structures can not be accurately estimated. This left us with the 31 SNR data set, referred to as S1 in further text. While all the data in S1 have associated integrated flux density errors, only 7 points have associated diameter errors. To calculate error in Σ we need both flux density errors and diameter errors. Table 3 from F08 presents flux densities, diameters and associated errors for 10 SNRs observed with MERLIN in 1992 (not necessarily listed in Table 2 of F08). We used these 1992 measurements of flux densities, diameters and associated errors; this sample is further referred to as S2. For elliptical sources we calculated the mean geometric diameter (for both S1 and S2). The fits of non-weighted vertical and orthogonal offsets for S1, and non-weighted and weighted vertical and orthogonal offsets for S2 are presented in the next Section. In Table 1 we present the range of relevant quantities for S1 and S2 samples.

3. Fitting

The standard fitting procedure in the $\Sigma - D$ plane based on the vertical (parallel to y-axis) χ^2 regression has been used for calibration of empirical $\Sigma - D$ relations. Recently, Bandiera & Petruk (2010) have used a different method – regression analysis with two independent variables – diameter D , and the density of environment n_0 . In this paper, we stay with one independent variable D (or Σ), but change fitting

²Multi-Element Radio Linked Interferometer Network

Table 1: Summary characteristics of the selected samples (the number of sources in sample and range of relevant quantities). The adopted M82 distance is 3.2 Mpc (F08) which provides a linear size equivalent to 1 mas \equiv 0.0155 pc (as used in F08).

	S1	S2
N^a	31	10
S^b [mJy]	[0.099, 19.435]	[0.72, 39.01]
L [Js ⁻¹ Hz ⁻¹]	$[1.21 \times 10^{17}, 2.38 \times 10^{19}]$	$[8.82 \times 10^{17}, 4.78 \times 10^{19}]$
D [pc]	[0.64, 6.2]	[0.205, 2.25]
Σ [Wm ⁻² Hz ⁻¹ sr ⁻¹]	$[9.24 \times 10^{-19}, 4.16 \times 10^{-15}]$	$(6.42 \times 10^{-17}, 1.22 \times 10^{-13})$

Notes: ^a The number of sources in sample; ^b Integrated flux density.

procedure from vertical to orthogonal offsets. Dependence on n_0 is important for $\Sigma - D$ analysis. M82 SNRs evolve in denser environment (Chevalier & Fransson 2001, Arbutina & Urošević 2005), but variation in the ambient density certainly exists. This is consistent with observations of structural evolution and wide range in expansion velocities of individual SNRs in M82 (e.g. F08, Pedlar et al. 1999, McDonald et al. 2001, Beswick et al. 2006 and Fenech et al. 2010). Variation in expansion velocities is probably constrained by the differences in ambient density. This variation in density, if it is assumed that the SNRs are evolving along similar evolutionary tracks, probably does provide one of the key reasons for the moderately large scatter in the plotted $\Sigma - D$ correlation.

For description of the radio surface brightness evolution of an SNR, we should investigate $\Sigma - D$ correlation, while for the distance determination of SNRs we need $D - \Sigma$ correlation (see Green 2009). The starting point of our analysis is the requirement that the $D - \Sigma$ and $\Sigma - D$ fit parameter values are invariant within the estimated uncertainties. This can be achieved with the orthogonal regression fitting procedure. Here, we use both types of fitting: standard (vertical) and orthogonal, and compare the results.

Data fitting is performed numerically. We seek for the minimum of the χ^2 function using the simplex algorithm (O’Neil 1971). The fit parameter values and their errors, presented in Tables 2-4, are the mean values and associated standard deviations after 10000 bootstrap data re-samplings for each fit. When fitting with data errors, the vertical offsets are weighted with $\sigma_{y_i}^2$, while orthogonal offsets χ^2 are calculated as $\frac{(y_i - A - \beta x_i)^2}{\sigma_{y_i}^2 + (\sigma_{x_i} \beta)^2}$.

4. Analysis of fit statistics

At first glance, inspection of Figures 1 and 2 and Tables 2-4 leads to the conclusion that resulting fit parameters values are significantly influenced with the type of the fitting procedure. The $\Sigma - D$ slopes are obviously steeper for orthogonal offsets (Figures 1 and 2; Table 2). The approximately ”trivial” $\Sigma - D$ slope ($\beta \approx 2.4$) is transformed into a very steep slope ≈ 3.9 for the S1 sample of 31 SNRs (Table 2). Also, for the poorer sample with respect to the number of objects (10 S2 SNRs), steeper slopes are obtained, but the differences are not so huge as in the case of the larger sample (see Table 2). On the other hand, $D - \Sigma$ slopes are approximately the same in both fitting procedures (see Table 4). This is due to a rather small span of diameters (one order of magnitude) in comparison to the span of surface brightnesses (four orders of magnitude). This leads to flatter slopes which results in similar lengths of vertical and orthogonal offsets giving similar fit parameters.

For the proper $\Sigma - D$ analysis, the $L - D$ correlation should be checked. If the $L - D$ correlation does not exist, the trivial $\Sigma \propto D^{-2}$ form should not be used (Arbutina et al. 2004). The statistics of $L - D$ correlations for both M82 samples are rather poor. For the S2 sample, this is because of the relatively low coefficient of correlation and a small number of objects in the sample, while for the S1 sample, because of a very low coefficient of correlation. The coefficient of correlation r is calculated using the following equation:

$$r = \frac{\sum_i (x_i - \bar{x})(y_i - \bar{y})}{\sqrt{\sum_i (x_i - \bar{x})^2} \sqrt{\sum_i (y_i - \bar{y})^2}}. \quad (2)$$

Finally, based on the poor statistical results of the $L - D$ fits (Table 3) it can be concluded that both extracted samples show a high degree of scattering.

5. Monte Carlo simulations

We performed a set of Monte Carlo simulations to estimate the influence of the survey sensitivity selection effect on the $\Sigma - D$ slope for M82 sample (31 SNRs). In both fitting procedures (vertical and orthogonal) we used the algorithm described below.

5.1. Vertical offsets

Monte Carlo simulations are similar to those described in Paper I. First, we determined the empirical $\log \Sigma$ standard deviation from the best fit line, assuming $\log D$ as the independent variable. We then selected an interval in $\log D$ between 0.65 – 100 pc. This interval is then sprinkled with random points of the same $\log D$ density as that of the real data.

The simulated points, that lie on the $\log D$ axis, are then projected onto a series of lines at different slopes (in steps of 0.1 from 1.5 to 4.5). Each of these lines passes through the extreme upper left hand end of the best fit line to the real data. We also added Gaussian noise in $\log \Sigma$, which is related to the scatter of the real data by a parameter called "scatter". A scatter of 1 corresponds to the same standard deviation as that of the real data.

An appropriate sensitivity cutoff is applied to the simulated data points, selecting points above the sensitivity line (for simplicity, we assumed a sensitivity line that passes through the real data point of the lowest brightness). This is done 1000 times for each simulated slope and a least squares best fit line (vertical regression) is generated for artificial samples.

In Table 5, the first column lists the scatter and second column shows the value of the simulated slope. Columns 3-6 are for vertical offsets, the mean and standard deviation of the best fit slopes for the generated samples and mean and standard deviation of the best fit slopes for sensitivity selected generated samples, respectively. In the same manner, columns 7-10 list the properties for orthogonal offsets. Figure 3 shows one of our Monte Carlo generated samples for vertical offsets at 5 GHz with a scatter of 1 and the simulated slope of 2.4.

5.2. Orthogonal offsets

We calculated standard deviation of data from the data best fit line using the orthogonal offsets. Then we have generated random diameters as described above. The points are then projected onto the simulated slope line. Then we added the Gaussian noise to the simulated points in orthogonal direction from the simulated slope line, as:

$$D_{\text{noise}} = D_{\text{proj}} \pm \frac{n_{\text{orth.}}}{\sqrt{1 + \frac{1}{b^2}}}, \quad \Sigma_{\text{noise}} = \Sigma_{\text{proj}} \pm \frac{n_{\text{orth.}}}{1 + b^2}, \quad (3)$$

with $n_{\text{orth.}}$ being the noise in the orthogonal offset direction and b the simulated slope. All artificial samples are fitted using orthogonal fitting procedure repeated 1000 times. The results of Monte Carlo simulations for orthogonal offsets are presented in Figure 3 (for slope $\beta = 3.9$) and Table 5.

6. Discussion

By contrast to the standard (vertical) fitting, the orthogonal regression procedure leads to a significant change in the slope of the $\Sigma - D$ relation from 2.4 to 3.9 (Table 2). The latter is a steep empirical slope, very far away from the trivial one ($\beta \approx 2$), and between theoretical predictions for the energy conserving phase of an SNR evolution ($\beta = 3.5$ and $\beta = 4.25$), obtained by Duric & Seaquist (1986) and Berezhko & Völk (2004), respectively. The inverted slope value ($1/3.9 \approx 0.26$) is approximately the same as the value obtained by $D - \Sigma$ fitting. Thus, for the orthogonal fitting procedure, $D - \Sigma$ and $\Sigma - D$ fit parameters values are invariant within the estimated uncertainties (see Tables 2, 4). A careful inspection of Table 4 leads to the conclusion that both fitting procedures provide similar $D - \Sigma$ slopes. Therefore, in case of M82 SNRs, instead of using the more complicated orthogonal regression method, one can find $D - \Sigma$ slope by the standard (vertical) fitting and after that invert it to find a valid $\Sigma - D$ slope. This supports a suggestion to use $D - \Sigma$ relation given by Green (2009). This is possible because of the narrow span of diameters for M82 SNRs (one order of magnitude) in comparison with the wide span of brightnesses (four orders of magnitude). If these spans are similar, the orthogonal procedure has to be used for the useful $D - \Sigma$ regression, too.

Based on the $L - D$ analysis (Table 3) it can be concluded that corresponding correlations are very poor. A large scatter in the data is evident and hence the correlation coefficients are low. On the other hand, some poor trends in the LD plane are visible but the moderately large level of scattering (or a small number of objects) in analyzed samples could not provide any valid conclusion about these trends (see Figures 1 and 2, second panel). There are observed differences in the expansion velocities of the SNRs in M82 (see F08 and references therein). This implies either that they are on different evolutionary tracks (connected with different initial energy of explosion), and/or expanding into different density regions, or as a consequence may be in different phases of SNR evolution. Consequently, a relatively large data scatter can be explained by the above noted influences.

When presenting fit parameter values in the tables, we have given the ratio of weighted sum of square residuals (offsets) and number of degrees of freedom ($WSSR/ndof$). The probability Q of obtaining larger weighted sum of square residuals is also presented. While for non-weighted offsets $WSSR/ndof$ and Q values are of no practical importance and are calculated only for the sake of completeness, they show that weighted fits are not statistically justified ($Q \gtrsim 0.001$ and $WSSR/ndof \sim 1$, when the scatter is of the order of ~ 1 standard deviation).

Arbutina & Urošević (2005) argued that SNRs of different types can be found along more or less parallel tracks in the ΣD plane. The tracks are presumably defined by the density of the surrounding environment in which SNRs evolve. Inspection of Table 5 shows that for scatters larger than 1, slopes of the $\Sigma - D$ relation are seriously under the influence of the sensitivity cutoff. This implies that for a reliable calibration of the $\Sigma - D$ relation, compact samples should be used (SNRs with similar initial properties evolving in similar environments). This criteria is probably satisfied for the M82 SNR sample consisting of young SNRs that evolve in dense environment of M82 starburst region. The latter conclusions may be valid if all SNRs have entered the energy conserving (Sedov) phase. The exact phase of evolution remains the main uncertainty for M82 SNRs. At least one compact SNR 43.3+59.2 has an exponent m , from the dynamical law $R \propto t^m$, ≥ 0.68 implying the free expansion (Beswick et al. 2006). Chevalier & Fransson (2001), on the other hand, argue that M82 SNRs may even be in the radiative phase.

For the simulated data scatter of 1, that should resemble the real scatter of the data, the slope of the $\Sigma - D$ relation is not severely biased by the sensitivity cutoff. Similar conclusion is drawn from the Monte Carlo sensitivity related simulations in Paper I. They used the M82 data sample of Huang et al. (1994),

collected with the Very Large Array, while the M82 sample analyzed in this work was recorded with the MERLIN measurements. This resulted in somewhat different sensitivity lines but nevertheless both studies came up with similar conclusions.

Monte Carlo simulations are carried out for the purpose of checking the completeness of the M82 SNR sample. Objects with low surface brightnesses can not be detected because they are affected by the survey sensitivity selection effect. By simulating this effect, we tried to find out whether our sample (i.e. corresponding $\Sigma - D$ slope) is representative for M82 SNR population or not. Inspection of Table 5, when scatter is generated by vertical offsets, show that sensitivity selection effect makes the observed $\Sigma - D$ slopes shallower. The result is identical to the one obtained in Paper I. When scatter is generated by the orthogonal offsets, the sensitivity line does not cut a significant number of artificial objects located in lower-left part of the field. In scatter 1 scenario, the sensitivity cutoff does not affect $\Sigma - D$ slope (see Table 5). A very interesting situation arises in the simulation of the orthogonal scatter 2 scenario. The $\Sigma - D$ slopes are changed significantly. The lower-left part of artificial samples is cut by the sensitivity line when scatter is high (higher than real one) and the slopes of relations become shallower. Based on the analysis of the results of simulations presented (Table 5), we believe that the orthogonal scatter 1 scenario is more likely for two reasons: (1) the slope ($\beta = 3.9$) is obtained by the orthogonal procedure that gives the invariant $\Sigma - D$ and $D - \Sigma$ slopes, and (2) scatter is generated by the orthogonal offsets and corresponds to the real scatter in observed data-set. We conclude that sensitivity selection effect does not have a major impact on the $\Sigma - D$ slope for M82 SNRs.

With $D - \Sigma$ and $\Sigma - D$ fit slopes being invariant within the estimated uncertainties in the orthogonal fitting procedure, assuming a relatively complete sample, the $\Sigma \propto D^{-3.9}$ relation for M82 SNRs could potentially describe the evolution of young SNRs in the energy conserving phase of their evolution, and this relation might be useful for estimating distances to such SNRs. The problem that remains is the coupling of the evident data scattering in F08 SNR sample and a small number of objects for which reliable statistics can be done. Another problem is that most of the sources do not show significant flux density variation (Kromberg et al. 2000), implying trivial physical relation $L_\nu \approx \text{const}$. Some sources, like 41.30+59.6 show flux increase, rather than decrease (F08). Therefore the $\Sigma - D$ relations obtained in this paper should be used with caution.

Finally, some compact radio objects in M82 may not be SNRs, as proposed by Seaquist & Stanković (2007). They analyzed compact nonthermal radio objects and concluded that some of them are probably the so-called Wind Driven Bubbles (WDBs) due to the lack of observed time variability in most of the sources, implying ages greater than expected for SNRs. However, the recent detection of γ radiation from M82 (Abdo et al. 2010) confirms standard opinion that radio objects in M82 are indeed SNRs. The strong shock waves of young SNRs are necessary for the efficient production of cosmic rays by the so-called diffuse shock acceleration (DSA) mechanism. The inverse Compton scattering of the background electromagnetic radiation by the cosmic ray electrons (leptonic model) or a decay of neutral pions, mainly produced by cosmic ray protons during the interaction with the gas (hadronic model) represent two basic mechanisms for production of γ rays. WDBs probably do not represent proper sites for the production of γ rays, due to slower shock waves in comparison to shock waves of young SNRs.

7. Conclusions

We suggest the orthogonal regression procedure to be used for obtaining empirical $\Sigma - D$ relations. In that case the values of parameters obtained from fitting of $\Sigma - D$ and $D - \Sigma$ relations are invariant within estimated uncertainties. Alternatively, if a data span in Σ covers more orders of magnitude than a data span in D , fitting of the $D - \Sigma$ relation with vertical offsets can give β that resemble the slope fitted with either $\Sigma - D$ or $D - \Sigma$ orthogonal offsets. The steep $\Sigma - D$ slope ($\beta = 3.9$) is obtained when fitting the orthogonal regression to the updated M82 SNR sample. The results of our Monte Carlo simulations suggest that this slope is probably free of the sensitivity selection effect. Moreover, it is closer to the updated theoretically derived slopes for the energy conserving phase of SNR evolution. The relation $\Sigma \propto D^{-3.9}$ could represent the average evolutionary track for SNRs in M82, and could potentially be used for estimating the distances of young SNRs expanding in dense environment. However, data scattering and, more importantly, a relatively small number of objects in the analyzed samples constrain the reliability of this relation. Due to this, the obtained $\Sigma - D$ relations should be used with caution. More observations and better theoretical description are necessary for deeper understanding of the radio evolution of these SNRs.

The authors would like to thank Dragana Momić for reading the manuscript and the anonymous referee for valuable comments that improved the quality of this paper. This work is part of the Projects No. 146003 and 146012 supported by the Ministry of Science and Environmental Protection of Serbia.

References

- Abdo et al. 2010, *ApJ*, 709, L152
- Arbutina, B., Urošević, D., Stanković, M. & Tešić, Lj. 2004, *MNRAS*, 350, 346
- Arbutina, B. & Urošević, D. 2005, *MNRAS*, 360, 76
- Bandiera, R. & Petruk O. 2010, *A & A*, 509, A34
- Berezhko, E.G. & Völk, H.J. 2004, *A & A*, 427, 525
- Beswick, R. J. et al. 2006, *MNRAS*, 369, 1221
- Case, G. L. & Bhattacharya, D. 1998, *ApJ*, 504, 761
- Chevalier, R. A. & Fransson, C. 2001, *ApJ*, 558, L27
- Chomiuk, L. & Wilcots, E.M. 2009, *AJ*, 137, 3869
- Clark, D.H. & Caswell, J.L. 1976, *MNRAS*, 174, 267
- Duric, N. & Seaquist, E.R. 1986, *ApJ*, 301, 308
- Fenech, D.M., Muxlow, T.W.B., Beswick, R.J., Pedlar, A. & Argo, M.K. 2008, *MNRAS*, 391, 1384 (F08)
- Fenech, D., Beswick, R., Muxlow, T. W. B., Pedlar, A. & Argo, M. K. 2010, *astro-ph/1006.1504*
- Green, D. A. 1984, *MNRAS*, 209, 449

- Green, D.A. 2009, *Bull. Astr. Soc. India*, 37, 45
- Guseinov, O.H., Ankay, A., Sezer, A. & Tagieva, S.O. 2003, *Astron. Astrophys. Transactions*, 22, 273
- Huang Z. P., Thuan T. X., Chevalier R. A., Condon J. J. & Yin Q. F. 1994, *ApJ*, 424, 114
- Kronberg P. P., Sramek R. A., Birk G. T., Dufton Q. W., Clarke T. E. & Allen M. L. 2000, *ApJ*, 535, 706
- McDonald, A. R., Muxlow, T. W. B., Pedlar, A., Garrett, M. A., Wills, K. A., Garrington, S. T., Diamond, P. J. & Wilkinson, P. N. 2001, *MNRAS*, 322, 100
- McDonald, A. R., Muxlow, T. W. B., Wills, K. A., Pedlar, A. & Beswick, R. J. 2002, *MNRAS*, 334, 912
- Milne, D.K. 1970, *Austral. J. Phys.* 23, 425
- Milne, D.K. 1979, *Austral. J. Phys.* 32, 83
- Muxlow, T. W. B., Pedlar, A., Wilkinson, P. N., Axon, D. J., Sanders, E. M. & de Bruyn, A. G. 1994, *MNRAS*, 266, 455
- O’Neil R. 1971, *Journal of the Royal Statistical Society Series C (Applied Statistics)*, 20(3), 338-345
- Poveda, A. & Woltjer, L. 1968, *AJ*, 73(2), 65
- Pedlar, A. Muxlow, T. W. B., Garrett, M. A., Diamond, P., Wills, K. A., Wilkinson, P. N. & Alef, W. 1999, *MNRAS*, 307, 761
- Seaquist, E.R. & Stanković, M. 2007, *ApJ*, 659, 347
- Urošević, D. 2002, *Serb. Astron. J.*, 165, 27
- Urošević, D., Pannuti, T. G., Duric, N. & Theodorou, A. 2005, *A & A*, 435, 437 (Paper I)
- Xu, J.-W., Zhang, X.-Z. & Han, J.-L. 2005, *Chin. J. Astron. Astrophys.*, 5, 165

Table 2: The $\Sigma - D$ relation.

fit	$\log A$	$\Delta \log A$	β	$\Delta \beta$	Q	$WSSR/ndof$	$\sqrt{WSSR/ndof}$
The sample of 10 SNRs from Table 3 in F08, $r = -0.924164$, $r^2 = 85.407974\%$.							
Ver. os.	-15.2842	1.48035e-01	3.00753	0.43692	9.92070e-01	1.92172e-01	4.38374e-01
Ver. os. w.	-14.9625	1.99015e-01	2.88255	0.41673	0.00000e+00	2.08336e+02	1.44338e+01
Ort. os.	-15.2874	1.56158e-01	3.60747	0.52914	9.99999e-01	1.62385e-02	1.27430e-01
Ort. os. w.	-14.9921	1.82236e-01	3.08412	0.47155	1.07173e-201	1.19871e+02	1.09485e+01
The sample of 31 SNRs from Table 2 in F08, $r = -0.782763$, $r^2 = 61.271836\%$.							
Ver. os.	-15.7409	2.01064e-01	2.41576	0.43166	9.99967e-01	2.71169e-01	5.20739e-01
Ort. os.	-15.2535	1.87001e-01	3.85631	0.43339	1.00000e+00	2.58510e-02	1.60783e-01

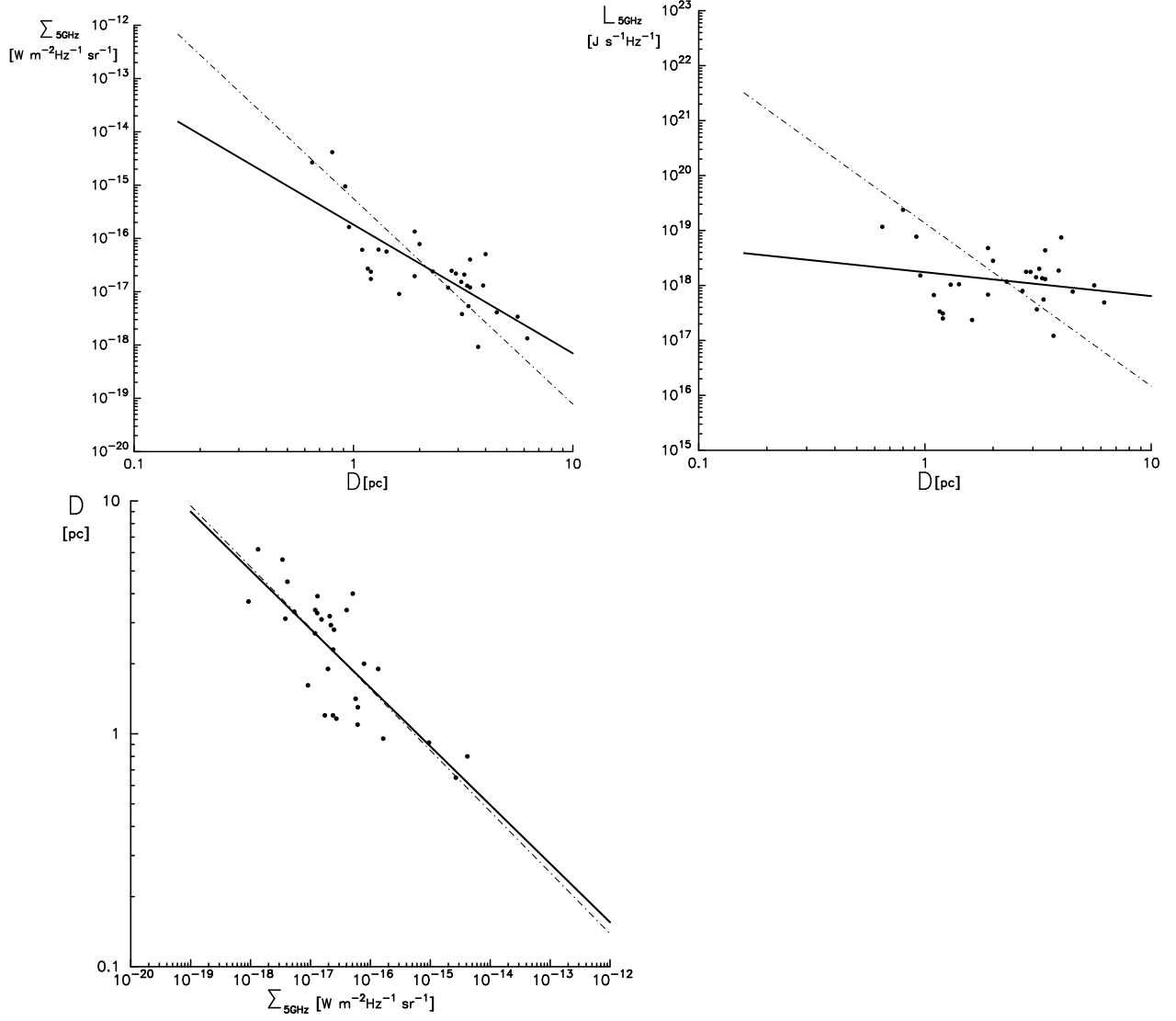


Fig. 1.— Data from Table 2 in F08 (31 SNRs). Thick solid line – non-weighted vertical offsets; dashed-dotted line – non-weighted orthogonal offsets.

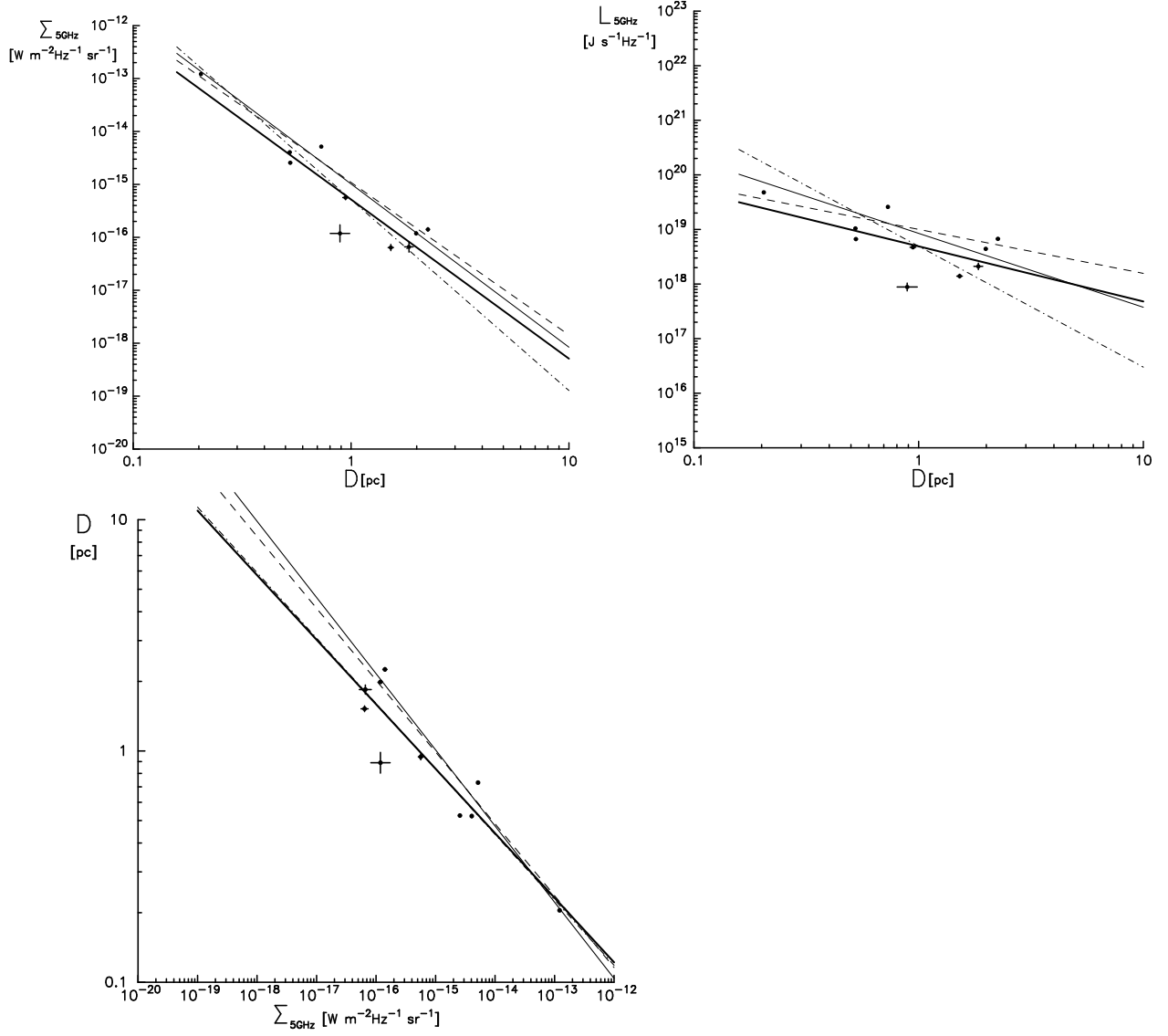


Fig. 2.— Data from Table 3 in F08 (10 SNRs). The errors are plotted for all points. Thick solid line – non-weighted vertical offsets; dashed line – weighted vertical offsets; dashed-dotted line and thin solid line are for the non-weighted and weighted orthogonal offsets, respectively.

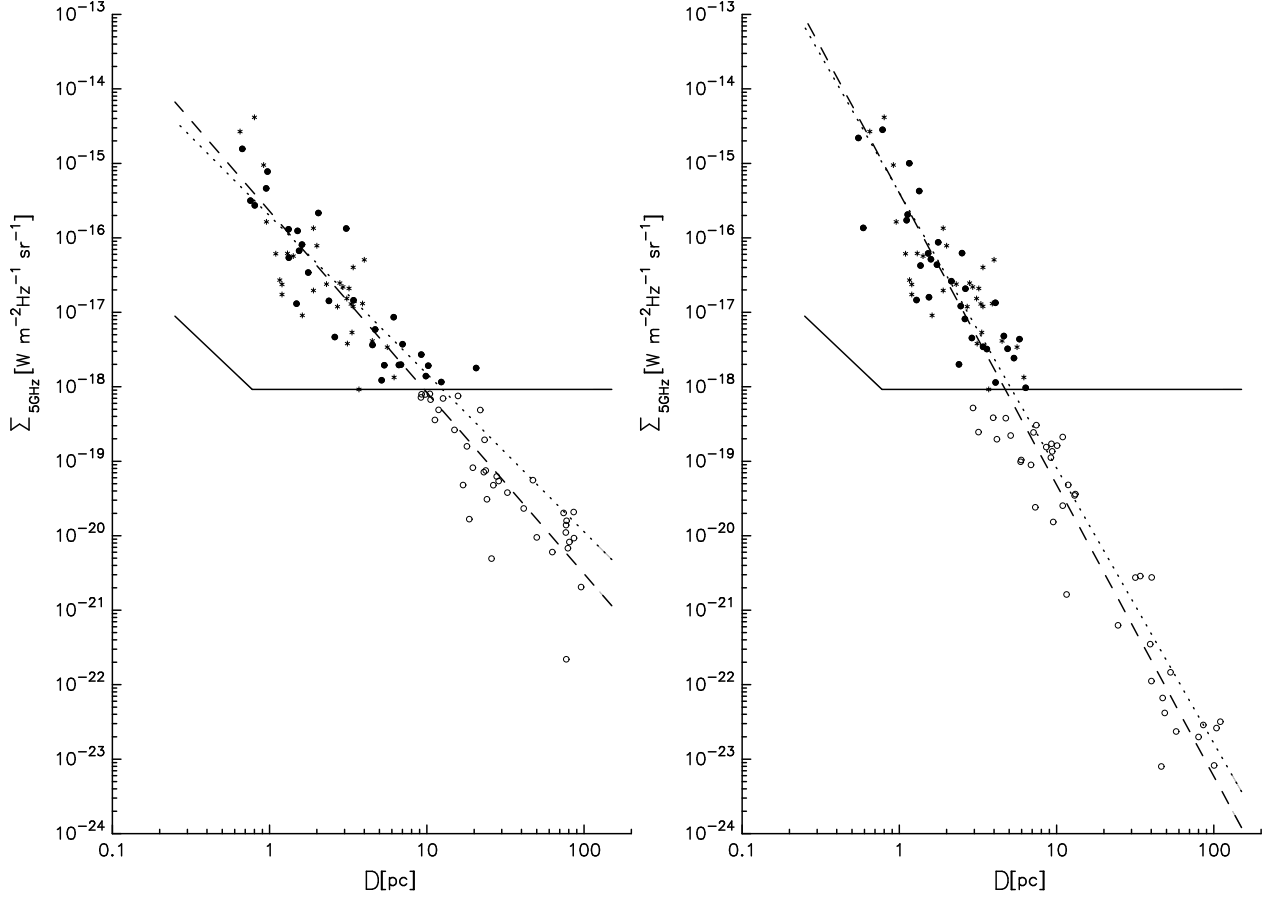


Fig. 3.— The Monte Carlo generated sample at 5 GHz for a scatter of 1. M82 data points (31 SNRs, signed by asterisks) are plotted together with the sensitivity (solid) line; artificially generated points are plotted above (filled circles) and below (open circles) this line. Dashed line – fit before selection; dotted line – fit after selection. Left – vertical offsets for a simulated slope of 2.4; right – orthogonal offsets for a simulated slope of 3.9.

Table 3: The $L = BD^{-\delta}$ relation.

fit	$\log B$	$\Delta \log B$	δ	$\Delta \delta$	Q	$WSSR/ndof$	$\sqrt{WSSR/ndof}$
The sample of 10 SNRs from Table 3 in F08, $r = -0.641483$, $r^2 = 41.150074\%$							
Ver. os.	18.6909	1.40852e-01	1.01038	0.43436	9.92093e-01	1.92008e-01	4.38187e-01
Ver. os. w.	19.0008	2.31966e-01	0.80511	0.57985	0.00000e+00	1.62263e+03	4.02818e+01
Ort. os.	18.6929	3.11494e-01	2.21533	0.95097	9.99888e-01	5.97075e-02	2.44351e-01
Ort. os. w.	18.9292	2.20137e-01	1.35415	0.82877	0.00000e+00	8.40500e+02	2.89914e+01
The sample of 31 SNRs from Table 2 in F08, $r = -0.236428$, $r^2 = 5.589839\%$							
Ver. offst.	18.2409	2.01469e-01	0.43333	0.43048	9.99971e-01	2.68603e-01	5.18269e-01
Ort. offst.	19.1334	7.52688e-01	2.96520	1.40621	1.00000e+00	7.25849e-02	2.69416e-01

A. On-line material: Results of Monte Carlo simulations

Table 4: The $D - \Sigma$ relation.

fit	coef.	$\Delta\text{coef.}$	$1/\beta$	$\Delta(1/\beta)$	Q	$WSSR/ndof$	$\sqrt{WSSR/ndof}$
The sample of 10 SNRs from Table 3 in F08, $r = -0.924164$, $r^2 = 85.407974\%$							
Ver. os.	-4.26141	5.54597e-01	0.27896	0.03736	9.99999e-01	1.74798e-02	1.32211e-01
Ver. os. w.	-4.66426e	6.73978e-01	0.31067	0.04486	0.00000e+00	2.80880e+02	1.67595e+01
Ort. os.	-4.32109e	5.48758e-01	0.28290	0.03697	9.99999e-01	1.61987e-02	1.27274e-01
Ort. os. w.	-4.93663	6.22588e-01	0.32945	0.04178	2.32472e-200	1.19097e+02	1.09131e+01
The sample of 31 SNRs from Table 2 in F08, $r = -0.782763$, $r^2 = 61.271836\%$.							
Ver. os.	-3.83090	4.62411e-01	0.25182	0.02793	1.00000e+00	2.75240e-02	1.65904e-01
Ort. os.	-4.00880	5.02672e-01	0.26253	0.03021	1.00000e+00	2.58590e-02	1.60807e-01

Table 5: The results of Monte Carlo simulations

Scatter	The slope that is simulated	Vertical offsets				Orthogonal offsets			
		Mean simulated slope	Standard deviation of mean simulated slope	Mean slope after selection	Standard deviation of slope after selection	Mean simulated slope	Standard deviation of mean simulated slope	Mean slope after selection	Standard deviation of slope after selection
1.0	1.500000	1.500696	0.099013	1.286365	0.109226	1.497463	0.055816	1.497168	0.055705
1.0	1.600000	1.600147	0.104393	1.349833	0.123326	1.598297	0.057974	1.587014	0.058188
1.0	1.700000	1.699489	0.099988	1.426584	0.131765	1.702749	0.060101	1.683068	0.067908
1.0	1.800000	1.802722	0.101126	1.507596	0.148833	1.804823	0.063576	1.782269	0.076331
1.0	1.900000	1.899529	0.101864	1.576387	0.156577	1.901645	0.065447	1.878356	0.082454
1.0	2.000000	1.997602	0.096299	1.672339	0.168350	2.003504	0.066718	1.979787	0.094530
1.0	2.100000	2.101995	0.101180	1.751897	0.183618	2.097585	0.069813	2.071091	0.112198
1.0	2.200000	2.203092	0.101992	1.836862	0.198541	2.201668	0.070944	2.182622	0.121677
1.0	2.300000	2.298177	0.100645	1.911342	0.212355	2.297719	0.078436	2.278483	0.139566
1.0	2.400000	2.402304	0.099143	2.005975	0.228506	2.402684	0.080858	2.384728	0.146849
1.0	2.500000	2.500295	0.100127	2.098402	0.243022	2.504435	0.081318	2.481287	0.165271
1.0	2.600000	2.602096	0.101548	2.172323	0.261917	2.600812	0.088288	2.576799	0.184526
1.0	2.700000	2.702694	0.101349	2.266196	0.287042	2.704265	0.085594	2.675869	0.204002
1.0	2.800000	2.799537	0.100410	2.340753	0.298422	2.799311	0.090789	2.784884	0.229936
1.0	2.900000	2.897140	0.098674	2.421775	0.310348	2.899872	0.095418	2.877078	0.238608
1.0	3.000000	2.996749	0.099588	2.498980	0.323027	3.003264	0.098458	2.979326	0.249424
1.0	3.100000	3.104522	0.098841	2.589717	0.345333	3.102771	0.102963	3.076613	0.290303
1.0	3.200000	3.202747	0.102624	2.688157	0.357554	3.204156	0.104733	3.179113	0.326909
1.0	3.300000	3.298963	0.099057	2.763613	0.362475	3.300337	0.106178	3.290091	0.310472
1.0	3.400000	3.402224	0.102481	2.839851	0.412462	3.405014	0.104106	3.377635	0.405915
1.0	3.500000	3.507588	0.104501	2.953550	0.443178	3.500932	0.107231	3.498262	0.398552
1.0	3.600000	3.601357	0.098950	3.027741	0.440752	3.603510	0.113465	3.603639	0.441060
1.0	3.700000	3.698463	0.102682	3.100663	0.431116	3.699302	0.115896	3.686992	0.517250
1.0	3.800000	3.800653	0.102899	3.198014	0.492386	3.809688	0.118302	3.789941	0.506556
1.0	3.900000	3.901953	0.100244	3.276876	0.484156	3.907993	0.121222	3.879406	0.624074
1.0	4.000000	3.997578	0.100347	3.371390	0.524299	4.003947	0.128336	3.956310	0.633162
1.0	4.100000	4.098606	0.103149	3.451102	0.567184	4.101723	0.127667	4.003518	0.836152
1.0	4.200000	4.203367	0.099424	3.549554	0.561571	4.205925	0.131813	4.103016	0.918963
1.0	4.300000	4.296356	0.103596	3.563594	0.564266	4.301982	0.133642	4.140517	0.947753
1.0	4.400000	4.399762	0.102086	3.677029	0.617068	4.396678	0.136565	4.231672	1.092972
1.0	4.500000	4.500762	0.099421	3.754998	0.640986	4.513678	0.138215	4.261958	1.206376
2.0	1.500000	1.497074	0.101099	1.010993	0.208958	1.503948	0.123884	1.491782	0.120576
2.0	1.600000	1.601748	0.206268	1.059087	0.211039	1.611962	0.125516	1.565151	0.122074
2.0	1.700000	1.699103	0.206710	1.097170	0.225302	1.709634	0.127692	1.629440	0.129925
2.0	1.800000	1.815947	0.198277	1.148707	0.227667	1.806221	0.136550	1.718790	0.151350
2.0	1.900000	1.898634	0.205865	1.184780	0.240272	1.906057	0.140358	1.818100	0.177176
2.0	2.000000	2.003181	0.208126	1.229978	0.239254	2.001608	0.141960	1.909523	0.193236
2.0	2.100000	2.106723	0.196232	1.282816	0.266664	2.115680	0.149275	2.012858	0.243819
2.0	2.200000	2.195067	0.200040	1.317523	0.278585	2.214054	0.154374	2.100802	0.277017
2.0	2.300000	2.297552	0.198016	1.378041	0.304825	2.310805	0.166987	2.184658	0.346117
2.0	2.400000	2.402734	0.192766	1.457052	0.326163	2.403606	0.169570	2.268059	0.405243
2.0	2.500000	2.500341	0.191161	1.510620	0.345794	2.519952	0.178789	2.328069	0.539537
2.0	2.600000	2.603374	0.201804	1.553823	0.358145	2.606837	0.179346	2.382969	0.617191
2.0	2.700000	2.696222	0.194625	1.628281	0.407107	2.702147	0.182631	2.305122	0.883883
2.0	2.800000	2.802244	0.198338	1.671113	0.416296	2.818203	0.190096	2.292552	0.999156
2.0	2.900000	2.904717	0.209044	1.757733	0.452250	2.918469	0.191426	2.191101	1.186119
2.0	3.000000	3.000119	0.200248	1.794150	0.449686	3.009131	0.205601	2.091009	1.306820
2.0	3.100000	3.095304	0.199938	1.861154	0.493821	3.120773	0.203151	2.027416	1.389508
2.0	3.200000	3.206066	0.200175	1.928786	0.495782	3.210318	0.209492	1.922314	1.469364
2.0	3.300000	3.305481	0.191043	2.017072	0.513027	3.318200	0.220698	1.704367	1.569541
2.0	3.400000	3.397078	0.198111	2.045195	0.562483	3.406487	0.224814	1.631980	1.610402
2.0	3.500000	3.510252	0.208732	2.105675	0.588506	3.516766	0.231254	1.439036	1.648696
2.0	3.600000	3.602030	0.206381	2.150111	0.604538	3.619306	0.233198	1.341696	1.673103
2.0	3.700000	3.691687	0.201116	2.245178	0.687834	3.713207	0.232729	1.240939	1.677783
2.0	3.800000	3.814261	0.194869	2.285464	0.694195	3.822946	0.250042	1.173427	1.684988
2.0	3.900000	3.899518	0.198059	2.332963	0.720083	3.915391	0.253124	1.115622	1.664230
2.0	4.000000	4.007378	0.208750	2.446729	0.717167	4.025399	0.257137	0.951611	1.650998
2.0	4.100000	4.108197	0.209448	2.473150	0.788030	4.117051	0.254371	0.863239	1.593827
2.0	4.200000	4.203942	0.206663	2.561313	0.789212	4.232547	0.274843	0.830775	1.621492
2.0	4.300000	4.303620	0.199229	2.637333	0.854930	4.325485	0.272846	0.783813	1.597587
2.0	4.400000	4.399662	0.196009	2.689233	0.854584	4.413641	0.279349	0.608025	1.497785
2.0	4.500000	4.515249	0.199041	2.720509	0.910855	4.513320	0.282582	0.701798	1.558721